Field Demonstration of the Impact of Fractures on Hydrolyzed Polyacrylamide Injectivity, Propagation, and Degradation

Marat Sagyndikov[1,2]*, Randall Seright[3], Sarkyt Kudaibergenov[4], and Evgeni Ogay[2]

[1]Satbayev University, Almaty, Kazakhstan
[2]KMG Engineering LLC, Nur-Sultan, Kazakhstan
[3]New Mexico Institute of Mining and Technology
[4]Institute of Polymer Materials and Technology, Almaty, Kazakhstan

Summary

During a polymer flood, the field operator must be convinced that the large chemical investment is not compromised during polymer injection. Furthermore, injectivity associated with the viscous polymer solutions must not be reduced to where fluid throughput in the reservoir and oil production rates become uneconomic. Fractures with limited length and proper orientation have been theoretically argued to dramatically increase polymer injectivity and eliminate polymer mechanical degradation. This paper confirms these predictions through a combination of calculations, laboratory measurements, and field observations (including step-rate tests, pressure transient analysis, and analysis of fluid samples flowed back from injection wells and produced from offset production wells) associated with the Kalamkas oil field in Western Kazakhstan. A novel method was developed to collect samples of fluids that were back-produced from injection wells using the natural energy of a reservoir at the wellhead. This method included a special procedure and surface-equipment scheme to protect samples from oxidative degradation. Rheological measurements of back-produced polymer solutions revealed no polymer mechanical degradation for conditions at the Kalamkas oil field. An injection well pressure falloff test and a step-rate test confirmed that polymer injection occurred above the formation parting pressure. The open fracture area was high enough to ensure low flow velocity for the polymer solution (and consequently, the mechanical stability of the polymer). Compared to other laboratory and field procedures, this new method is quick, simple, cheap, and reliable. Tests also confirmed that contact with the formation rapidly depleted dissolved oxygen from the fluids—thereby promoting polymer chemical stability.

Introduction

The investment in chemicals during a polymer flood can amount to tens of millions to hundreds of millions of dollars. Thus, any polymer degradation (and consequently reduced polymer solution viscosity) can incur a substantial cost. Mechanical and oxidative degradation are two major concerns during a polymer flood (Maerker 1975; Seright 1983; Seright et al. 2009, 2010, 2021; Manichand et al. 2013; Seright and Skjevrak 2015; Jouenne et al. 2017). Straightforward calculations, coupled with laboratory results, reveal that mechanical degradation of hydrolyzed polyacrylamide (HPAM) polymers will be quite high during injection into unfractured vertical wells (Seright et al. 2009). In contrast, if a fracture is open at the injection well, calculations suggest that the increased rock-face area associated with the fracture reduces fluid velocities to the point that mechanical degradation of HPAM is no longer a concern (Seright et al. 2010; Manichand et al. 2013). (The fracture could be newly created, a previously induced hydraulic fracture, or an existing natural fracture.) A significant part of this paper is dedicated to testing/confirming this prediction in a field application. This confirmation required developing a method to back-produce polymer solutions without inducing further mechanical or oxidative degradation. As will be revealed in our literature review, most previous attempts to collect polymer from a reservoir have induced substantial degradation during the sampling/measurement process. In contrast, our method is quick, simple, cheap, and reliable.

Previous calculations (Seright et al. 2009; Van den Hoek et al. 2009; Seright 2017; Ma and McClure 2016) suggested that polymer injectivity into vertical wells would be unfeasible without open fractures. In contrast, others (Lotfollahi et al. 2016; Skauge et al. 2016; Åsen et al. 2019; Delamaide 2019) attempted to justify observed field polymer injectivities using controversial assumptions about HPAM rheology during radial flow (i.e., in unfractured vertical wells). This raises the question: "How do we know that we actually have a fracture intersecting our injection well?" In this paper, this question will be answered using a combination of calculations, laboratory tests of polymer rheology in porous media, and field tests using pressure transient analysis and step-rate tests.

An additional benefit from this study was confirmation that contact of HPAM solutions with the reservoir rock promoted polymer stability by removing dissolved oxygen. As will be shown, solutions that were back-produced from the injection well and those that propagated from an injector to a producer contained dissolved oxygen levels that were substantially lower than those of injected fluids. This finding is consistent with known geochemistry and results from other field tests (Seright et al. 2011; Manichand et al. 2013).

Literature Review

During a typical polymer flood, a high molecular weight partially HPAM significantly increases viscosity for the injected water, thereby reducing the water/oil mobility ratio and improving reservoir sweep efficiency (Lake 1989). However, HPAM solutions can experience significant viscosity losses through mechanical and oxidative degradation (e.g., Seright 1983; Seright et al. 2010; Seright et al. 2011; Seright and Skjevrak 2015). Thus, minimizing polymer degradation is key to successful polymer flooding.

Viscosity/Molecular Weight of Produced Polymer Solutions. If polymer solutions are produced from reservoir production wells with no loss of viscosity or molecular weight, that knowledge could comfort the operator that the polymer did not deteriorate by any degradation mechanism. Several field applications attempted to quantify polymer degradation of produced fluids and suggested severe loss of polymer molecular weight. A sampling of production wells at Daqing revealed ~80% viscosity loss for HPAM after traveling approximately 800 ft through the Daqing sand at 45°C (Zhang 1995; Shao et al. 2005; Wang et al. 2008a, 2008b). After 2–3 years of residence time in the Daqing reservoir, You et al. (2007) reported that polymer molecular weight decreased by 92% (from 19.8 million daltons to 0.89 million daltons), and the degree of hydrolysis increased from 28 to 36.2%. You et al. (2007) also reported that HPAM molecular weight decreased by 77.2% (from 17.3 million daltons to 3.94 million daltons), and the degree of hydrolysis increased from 22.3 to 38.2% upon flowing through the Shengli reservoir (70°C, 2–3 years residence time). After transiting the Shuanghe (Henan) reservoir (70°C, 2–4 years residence time), You et al. (2007) reported HPAM molecular weight decreased by 84.6% (from 15.2 million daltons to 2.35 million daltons), and the degree of hydrolysis increased from 23.7 to 59.5%. For HPAM produced from the Courtenay polymer flood (30°C), Putz et al. (2013) noted that the HPAM lost about one-half of its viscosifying ability. Manichand et al. (2013) reported that early efforts at characterization suggested an 83% decrease in polymer molecular weight afterflow through the Tambaredjo field (Suriname, 38°C). These losses seemed excessive, considering the temperatures of the fields. Previous laboratory work indicated that HPAM solutions should be quite stable, considering the conditions present in most low-temperature reservoirs (Shupe 1981; Yang and Treiber 2013; Moradi-Araghi and Doe 1987; Seright et al. 2011). So, the field observations are troubling because they raise questions about when and how polymer degradation occurred. If the polymer degraded during or shortly after injection, the polymer flood may not be viable. On the other hand, if degradation occurs at or near the production wells, the degradation has little or no negative impact. For the cases mentioned above, where pessimistic assessments of polymer degradation were made, it is prudent to ask whether an improved sampling method might result in less observed degradation (i.e., more in line with the predictions made from laboratory results).

Fortunately, Manichand et al. (2013) demonstrated that at least for the Suriname case, the observed degradation was an artifact of the old method used to sample and measure the viscosities of the produced polymer solutions. An improved method was introduced that used the traditional method of first flushing the sample cylinder from the bottom to the top and producing several cylinder volumes of fluid before closing the cylinder valves. However, in addition, after the cylinder arrived at the laboratory, a plastic attachment was placed at the bottom of the cup of the ultralow adapter of a Brookfield viscometer. Tubing was connected from the bottom of the sample cylinder to this plastic attachment on the viscometer. Then, nitrogen was introduced into the top of the sample cylinder to force the fluid sample into the viscometer cup. The flow was allowed to overflow from the top of the viscometer cup to flush out all oxygen. After this fluid overflow showed undetectable dissolved oxygen, the viscometer was turned on to measure the viscosity of the anaerobic sample. Using this improved sample collection and analysis method, they proved that the HPAM solutions propagated through 330 ft of the Tambaredjo reservoir with no significant degradation. Their work confirmed that although polymer solutions may have high dissolved oxygen levels upon injection, iron minerals in the formation quickly removed that oxygen. Oxygen-free polymer solutions can then readily dissolve iron during propagation through the reservoir. This dissolved iron (Fe^{2+}) is not detrimental to the polymer so long as oxygen is not redissolved in the solution (Seright and Skjevrak 2015). Thus, an effective sampling method must keep the sample anaerobic; otherwise, oxidation may mislead the operator that severe polymer degradation occurs. This is an important lesson that we incorporated in our methodology.

Laboratory Assessment of Mechanical Degradation. Many laboratory methods were developed to predict mechanical degradation in tubing, the near-wellbore zone, and under reservoir conditions (Maerker 1975; Morris and Jackson 1978; Seright 1983; API RP 63 1990; Noïk et al. 1995; Seright et al. 2009, Seright et al. 2011; Manichand et al. 2013; Puls et al. 2016; Jouenne et al. 2017; Åsen et al. 2019; Garrepally et al. 2020). A common feature of these methods is the determination of the viscosity of polymer solutions before and after the test. Tests were performed using field cores, sandpacks, outcrop cores, and blenders. These laboratory tests injected polymer solutions at different flow rates (flux or Darcy velocity) to model fluid velocities through perforations, the near wellbore, and within the reservoir. Assumptions made for different flow regimes (velocities) were often based on the Darcy radial flow equation. In contrast, most of the worldwide polymer flood projects injection in vertical wells occurs above the formation parting pressure (Seright et al. 2010; Van den Hoek et al. 2012; Seright 2017), where the linear flow was expected. (Here, in our terminology, "parting pressure" is simply the pressure at which a fracture or fracture-like feature opens. It may be the first time the fracture was created or alternatively that a fracture that was created previously but subsequently closed when the pressure was reduced.) To test and complement these ideas, there is considerable value in reviewing field experiments where polymer degradation was assessed directly using downhole sampling from a polymer injector (Xue et al. 2012; Puls et al. 2016), samples collected from an observation well near the injector (Morel et al. 2015), or from a polymer production well (Manichand et al. 2013).

Field Assessment of Mechanical Degradation. Field operators in Austria (Puls et al. 2016), Angola (Morel et al. 2015), China (Xue et al. 2012), and Suriname (Manichand et al. 2013) conducted field tests to assess polymer degradation near wellbore and deep in the formation by direct methods. These field cases used HPAM, which is the same type of polymer used in the Kalamkas field.

In the Austrian field test, the injected polymer solution was back-produced using a swabbing unit. In addition, swabbing was performed after injection. The test results showed that molecular weight decreased from 20 million daltons to 8 million daltons (60% degradation).

The Dalia (offshore Angola) field test collected bottomhole samples from a special observation well, which was drilled 80 m from a polymer injector. This observation well was located upstream of the polymer front (which was located using 4D seismic monitoring). A modular dynamic tester was tested onshore to confirm that the polymer solution did not suffer severe degradation during sampling. Based on onshore test results, the operator added precautions, such as using new valves, coated pipes (i.e., with Sulfinert™), flushing dead volumes with ultrapure nitrogen to remove oxygen, and careful flow rate control. The analyses of samples showed that the average degradation was 75% and polymer concentration was in the same range as the injected solution.

During a field test in China (Xue et al. 2012), downhole polymer solutions were recovered using coiled tubing and a nitrogen-assisted flowback technique. Direct measurements of the concentration and viscosity revealed that the polymer solution was degraded, with the viscosity of the polymer reduced to one-third of injected value. Initial viscosity was 21.5 cp and, after flowback from 0.24 m into the reservoir formation, was degraded to 7.7 cp.

The above field tests might be viewed as disheartening because so much polymer degradation was noted. However, one must ask whether the sampling method is the source of the apparent degradation. A field test in Suriname collected anaerobic polymer solution samples from production wells. Manichand et al. (2013) used a simple sampling procedure that allows collection of polymer samples from a well, introduction into a Brookfield viscometer, and viscosity measurement—all under anaerobic conditions. Viscosity measurements of samples revealed that the polymer solution effectively propagated from an injector to a producer (~330 ft) with no significant

degradation. In their case, based on analytical calculations, polymer solution injectivity was 61 times greater than expected for injection into an openhole completion, and the fracture area was roughly 61 times greater than that associated with an open hole. This area equated to a fracture that extended radially 20 ft from the well. By increasing the sandface area by a factor 61, the velocity when the polymer enters the formation is reduced in proportion, and as a consequence, the possibility of HPAM mechanical degradation is reduced.

Importance of Fractures. Because of a fear that fractures might cause severe channeling, one might desire to inject polymer solutions under conditions where fractures are not open near an injection well. However, in vertical injection wells, simple Darcy's law calculations reveal that without open fractures, polymer injection below the formation parting pressure will reduce injectivity (relative to water injection) by at least 80% (Seright et al. 2009). One can easily test this idea in any existing polymer flood field injector to prove its validity (Wang et al. 2008a; Manichand et al. 2013; Seright 2017). Consequently, it is commonly argued that all vertical polymer injection wells, and even most water injection wells have open fractures (Seright et al. 2010; Van den Hoek et al. 2009; Ma and McClure 2016). For horizontal wells, the necessity to inject polymer above the formation parting pressure is significantly less (Seright et al. 2009). Nevertheless, horizontal wells may still intersect fractures or fracture-like features (Seright et al. 2010; Dandekar et al. 2019). For those cases, fluid flow profiles should be used to identify the location of the fracture-like feature—and consideration can be given to the value of plugging this feature (e.g., using a gel treatment; Seright and Brattekas 2021).

Alternative Views of Polymer Injectivity and Mechanical Degradation. Much of the literature mentioned above argues that fractures or fracture-like features must be open during most/all previous field polymer floods where polymer solutions were injected into vertical wells. At the heart of this argument is the observation in most/all previous field polymer floods that the injectivity during polymer injection was not substantially different from that during previous water injection (Wang et al. 2008a, 2008b; Seright et al. 2010; Van den Hoek et al. 2009; Manichand et al. 2013; Seright 2017). For example, suppose a 10 cp Newtonian polymer solution is injected into a vertical well with no fractures. In that case, the Darcy equation predicts substantially lower injectivity (e.g., perhaps, roughly 10 times lower) than 1 cp water—especially because viscous behavior near the wellbore dominates flow resistance during radial flow. However, contrasting viewpoints have been argued in the literature.

Delamaide (2019) advocated an analytical method to estimate injectivity of HPAM solutions in vertical wells with no fractures. His model assumed shear-thinning rheology for HPAM solutions at near-wellbore velocities, which contradicts all experimental studies (Dauben and Menzie 1967; Hirasaki and Pope 1974; Maerker 1975; Seright 1983; Heemskerk et al. 1984; Seright et al. 2009, Seright et al. 2011; Jouenne et al. 2017). Thus, this model appears to use two opposing incorrect assumptions (i.e., no fractures and no shear-thickening behavior at high velocities) in an attempt to match observed field injectivities. Even with these assumptions, the author had difficulty matching observed field injectivities.

Skauge et al. (2016) performed radial and linear corefloods with HPAM solutions. They advocated that transient phenomena during radial flow caused substantial differences in polymer rheology in porous media that were not consistent with observations during linear flow. They suggested that these differences might explain why injectivities during polymer injection during field applications were not much lower than those during water injection. However, no calculations or analyses were performed to examine whether this suggestion was possible. In their work, throughout the full range of examined fluid velocities (0.01 to 40 ft/D), the apparent viscosity never fell below 80 cp. Thus, the injectivity loss could not be less than that of a 80 cp Newtonian fluid (Seright et al. 2010). Consequently, Skauge et al. (2016) arguments cannot quantitively rationalize observed field injectiviites as similar to water.

Åsen et al. (2019) argued that mechanical degradation of HPAM solutions in linear flow was significantly overestimated compared to that in radial flow. They predicted this result because during many cycles of injection of a single HPAM solution and reinjection into a linear core at a fixed velocity, they observed additional degradation during each cycle. They advocated that HPAM mechanical degradation would continue through up to 20 m during linear flow in porous media. In contrast, all other previous researchers (Maerker 1975; Seright 1983; Jouenne et al. 2017) consistently reported that HPAM mechanical degradation in linear flow was stabilized within 1 cm after entering the porous media. Close examination of the work of Åsen et al. suggests that their extended degradation results were due to oxidative degradation that occurred between each cycle of HPAM reinjection. Whether or not the results of Åsen et al. are accepted, all authors agree that HPAM that passed the sandface in radial flow would retain a significant resistance factor (e.g., 10 or greater for most practical HPAM solutions). Straightforward Darcy flow calculations consistently reveal that such polymer solutions would cause injectivity reductions (relative to water) of at least 80% in radial flow (Seright 1983; Seright et al. 2009).

Lotfollahi et al. (2016) performed a "mechanistic simulation" of polymer injectivity associated with selected field tests. Their model purported to include shear-thickening/viscoelastic behavior of HPAM solutions, shear thinning at low rates, presence of "junk" (undissolved particulates) in the polymer, polymer retention, and permeability reduction effects, but did not include the presence of fractures or fracture-like features (i.e., the radial flow was assumed around vertical polymer injection wells). The absence of fractures was assumed in the simulation, despite literature stating fractures were present in the modeled field (Matzen, Austria) and also despite a substantial initial water saturation (50%) and water breakthrough noted in the field. The work of Lottollahi et al. predicted very modest injectivity declines (no more than 50%) even for cases where the injected polymer viscosity was 10–100 cp and the polymer penetrated substantial fractions of the distance between injectors and producers. These predictions appear to be a strong violation of the Darcy equation, and the apparent contradictions were not addressed in the paper. One would have expected "mechanistic simulations" to explain such surprising results. "Black-box" predictions from a simulator are difficult to understand without first benchmarking against basic physics and common sense.

Tai et al. (2021) provided an improved method for calculating pressures in vertical polymer injection wells during simulations. They acknowledged that fractures might cause enhanced polymer injectivity. However, they pointed out that the concept of "pressure-equivalent radius" was commonly used to characterize bottomhole pressures (BHPs) and injectivities during simulations. In effect, the gridblock that contains the vertical injection well is assumed to contain a much larger effective wellbore radius than actually exists in any unfractured openhole completion. This procedure substantially increases the sandface area available to polymer entry into the porous medium—just as a fracture would. We respect this approach for accommodating observed injectivities during simulations. However, since the procedure assumes a circular "wellbore," it does not account for the directional nature of fractures and fracture growth.

Perhaps the great lengths that some have taken to deny the presence of fractures during polymer injection into vertical wells stem from government regulatory policies to "stay below the fracture or parting pressure during injection." These policies were understandably implemented to prevent fractures from developing that caused either severe channeling between injectors and producers or flow "out of zone" (i.e., breaking through flow barriers above or below the target formation). In the present paper and work, rather than to deny the presence of fractures, our approach is to accept and take advantage of the fact that fractures can have a very beneficial effect on injectivity,

sweep improvement, and reduction of mechanical degradation during HPAM injection into vertical wells (Seright 2017)—if the fractures do not extend too far to cause channeling problems.

One could argue that the most definitive way to establish that open fractures were responsible for mitigating HPAM mechanical degradation during a field project is to compare viscosities of back-produced solutions while injecting polymer below the formation parting pressure vs. above the parting pressure. Unfortunately, this suggestion is not practical in a real field setting, because the rates and injectivities are prohibitively low when the fractures (or fracture-like features) are not open during polymer injection into vertical wells. We have consciously looked for such a case throughout the literature and in discussions with field operators over the past 43 years—and have found none.

Novelty and Expected Value from the Current Work. The novelty in this work is in field demonstration of the correctness of previous conceptual ideas—(1) that the vertical HPAM injection wells contained fractures that were necessary for polymer injection, (2) that the fractures substantially reduced mechanical degradation, and (3) that injected polymer solutions were quickly stripped of dissolved oxygen (thereby promoting oxidative stability). These demonstrations have value in countering arguments by others (discussed above) that polymer injectivity into vertical wells could be acceptable without fractures. To our knowledge, this is the first published report demonstrating that backflowed HPAM samples from an injection well showed no detectable dissolved oxygen. [For the cases reported by Manichand et al. (2013), the polymer samples had traveled all the way from an injector to a producer.] Also, to our knowledge, this is the first published report demonstrating that backflowed samples from an injection well showed no HPAM mechanical (or oxidative) degradation. As mentioned in the literature review, previous reports of produced HPAM samples (from production wells, observation wells, and back-produced injection wells) commonly noted substantial degradation—possibly, because of the sampling methods used. Thus, the sampling method that we report here is also novel. We are certainly not claiming that oxidative and mechanical degradation are never a concern. Oxidative degradation will certainly be of concern if the temperature is high and efforts are not made to exclude oxygen from the polymer solutions (Seright and Skjevrak 2015; Seright et al. 2021). Also, mechanical degradation is certainly of concern if the wrong pumping, valving, choking, and filtration equipment are used. However, without a hope that polymers can be injected without mechanical or oxidative degradation, who would ever do a polymer flood in their right mind? We are trying to provide that hope.

The Kalamkas Oil Field

The tests in this paper are associated with the Kalamkas oil field, which is located in the Mangistau region of Western Kazakhstan. The field was discovered in 1976 and developed commercially since 1979 according to the Field Development Project (FPD) (Leibin and Ogay 1979). Oil and gas reservoirs were established in Jurassic deposits. Reservoirs mainly consist of sandstones deposited in deltaic, fluvial, and shallow marine environments.

The main geological and physical features of the reservoirs are highly layered heterogeneity and unfavorable oil/water viscosity (or mobility) ratio in reservoir conditions. The permeability ranges from 0.055 to 1.273 darcies. Physical and chemical properties (salinity, density, viscosity, and pH) of the Cretaceous and Jurassic formations' brines are quite similar **(Table 1).** The oil viscosity is at least 16 cp at reservoir temperature (38–43°C).

Parameter	Jurassic Formation Brine (From the Production Well)		Cretaceous Formation Brine (Used for Polymer Dilution)	
	West Producer XX94	East Producer XX29	West PF	East PF
pH	6.1	6.3	5.8	6.1
Density (g/cm^3)	1.089	1.081	1.072	1.080
Ca^{2+} content (ppm)	4,500	4,400	4,609	5,410.8
Mg^{2+} content (ppm)	2,640	2,400	2,189	2,432.0
Total salinity (TDS) (ppm)	136,211	123,445	98,722	108,913.7
Water type by Sulin (1946)	Cl-Ca	Cl-Ca	Cl-Ca	Cl-Ca
Water hardness (mg-eq/L)	445	420	410	470
Fe^{2+} content (ppm)	14	7.6	39.2	22.4
Fe^{3+} content (ppm)	32	37	1.4	2.8
Total suspended solids content (ppm)	Not measured	Not measured	14.0	12.0
Dissolved oxygen content (ppm)	Not measured	Not measured	0[1]	0[1]

[1]Dissolved oxygen content measuring with CHEMets® express tests shows the undetectable value (less than 0.025 ppm or 25 ppb).

Table 1—The Kalamkas field formation brine physical and chemical properties.

These factors explain nonuniform depletion and relatively low recovery factor for the Kalamkas oil field. To date, the water cut is significantly higher than expected considering the depletion of recoverable reserves **(Fig. 1).** (In this case, the depletion of recoverable reserves is defined as a percentage ratio of cumulative oil production and recoverable oil reserves.)

To improve hydrocarbon production and enhance oil recovery, a polymer flood pilot design started in 2011. The design of the injected polymer viscosity was based on the optimum economic output (i.e., net present value) according to reservoir modeling and feasibility studies, and on concepts presented in literature sources (Wang et al. 2008a, 2008b; Seright 2017). Pilot projects were conducted in two injectors in the West part since September 2014 and in four injectors in the East part of the field since March 2015. The West pilot is a 9-spot with a well spacing of 400 m as projected in FPD, and the East pilot (green triangles in **Fig. 2**) is an infilled 5-spot with a well spacing of 200 m. Except for oil recovery response, one of the main goals of the West and East pilots was to identify at which well pattern (existing or infilled) polymer flood shows the best result. As a result, the West pilot showed no injectivity loss; polymer injection unit uptime was high; sweep efficiency was increased (based on injection and production logging tests); water cut decreased to 8%; and oil
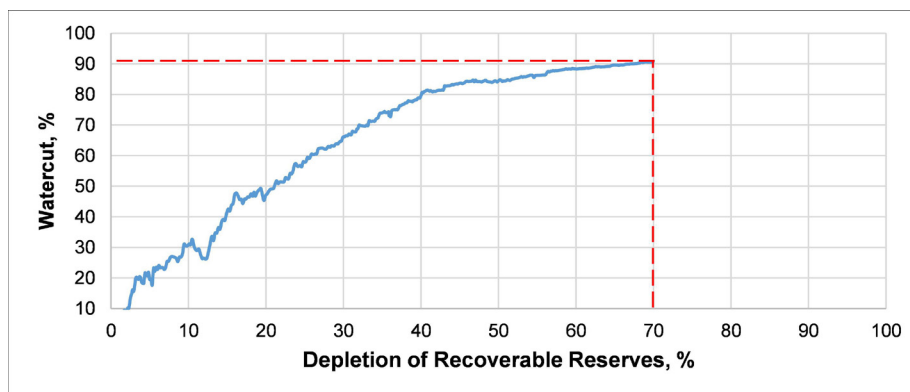
Fig. 1—History of the water cut vs. recoverable reserves depletion for the Kalamkas field.

production rates doubled. For this project, the estimated incremental recovery factor over waterflood was 9% (Sagyndikov et al. 2018). In contrast, the East pilot showed similar technological benefits, but the significant capital investment associated with the infill drilling led to a negative net present value. Consequentially, in 2017, the pattern was returned to water injection. Based on West and East pilot results, a larger polymer flood project was expanded to the existing 9-spot well patterns of the East part of the field using 11 injectors in 2018 and 2019 **(Fig. 2).** The new method to evaluate polymer mechanical degradation was tested in Injection Well 20 XX of the West Pilot area and Injection Wells XX24, XX41, XX37, and Producer XX87 of the East Extension area.

Table 1 provides the composition of the Cretaceous formation brine used in the polymer-solution injection process. This process includes preparing the mother solution and diluting it to the target concentration. The special production wells from a Cretaceous water reservoir supply the brine for West and East polymer flooding projects. We recognize that the formation salinities are quite high and that HPAM provides much more cost-effective viscosity in low-salinity brine than in high-salinity brine. Nevertheless, polymer flooding with HPAM under the conditions at Kalamkas still provides a substantial economic benefit. Furthermore, given the price and (lack of) availability of biopolymer (i.e., xanthan, scleroglucan, and schizophyllan), the use of HPAM is still more cost-effective than alternatives.

The dissolved oxygen level has been measured at the wellhead of the water production well and the storage water tank of the polymer injection unit using CHEMets® colorimetric tests. Test results reveal that the formation brine dissolved oxygen level is undetectable (less than 0.025 ppm or 25 ppb). This finding is consistent with the fact that Kalamkas oil reservoirs have a reducing environment due to iron-containing minerals up to 2 to 4% (Seright et al. 2011). As can be seen from the brine chemical analysis, the brine has high salinity and high content of divalent cations (Ca^{2+}, Mg^{2+}, and Fe^{2+}). The field brine iron content varies between 20 and 40 ppm. Consistent with the experimental work in Seright and Skjevrak (2015), the polymer solution viscosity losses at Kalamkas field conditions should be insignificant if the initial dissolved-oxygen concentration is 200 ppb or less.

Fig. 3 illustrates the polymer-solution main injection process and unit components. First, dry polyacrylamide powder was mixed with water in the polymer slicing unit. Subsequently, the dissolved polymer flowed to the maturation tank to achieve the required concentration
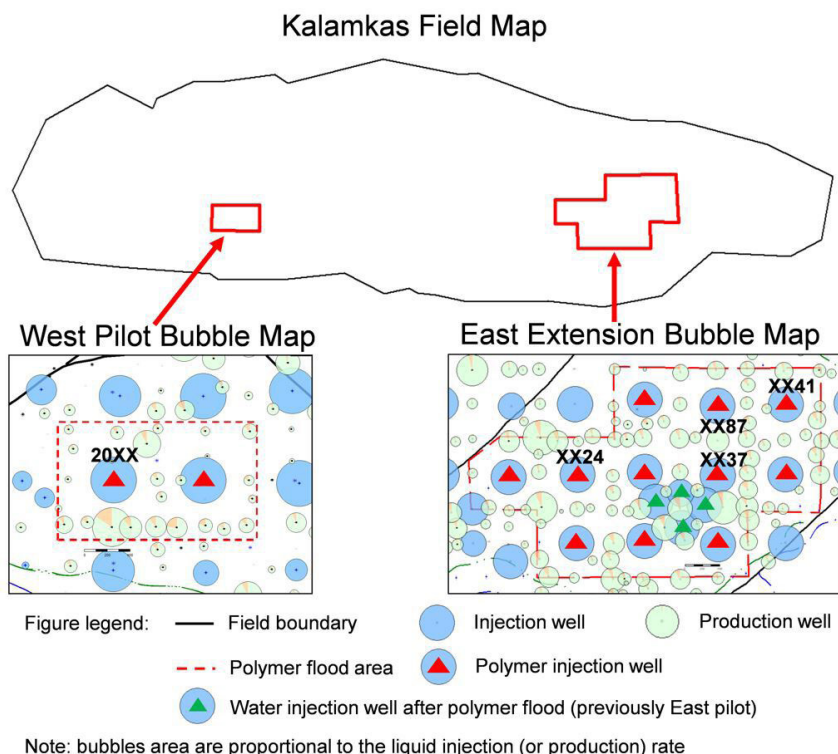
Fig. 2—Polymer flood project locations in the Kalamkas field.
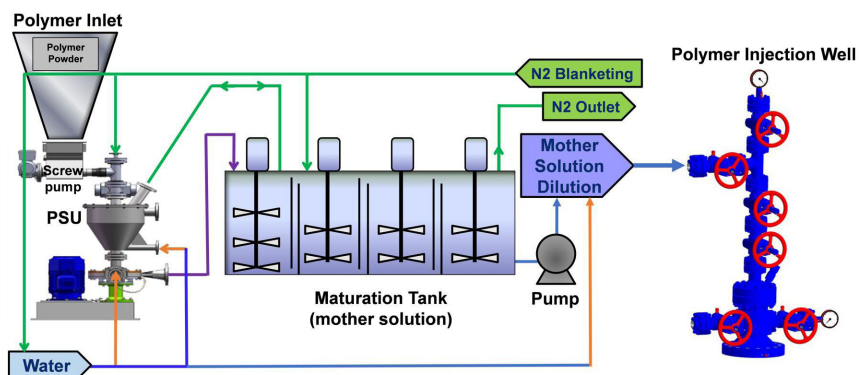
Fig. 3—Main components of the polymer solution injection unit.

and viscosity for the mother solution. The unit is completely isolated from air by nitrogen blanketing to protect the polymer solution from oxidative degradation. The next step is mixing the mother solution with brine to achieve the target viscosity, and then it is transferred by a low-shear pump to the injection well. For the East extension project, the mother solution polymer concentration is 15,000 ppm, and the injected polymer active concentration is 1,800 ppm, which can achieve, on average, 16–17 cp (at room temperature and shear rate 7.34 s^{-1}). An individual pump was used for each injection well. The partially HPAM (Polyacrylamide R-1) had a molecular weight of 15 million daltons and a hydrolysis degree of 16%. This polymer is a commercially available product. The chemical stability and good dissolving quality of the polymer were demonstrated during the experimental work of Seright and Skjevrak (2015) with polymers and conditions similar to those in our application.

Methods, Procedures, Equipment

Injector Back-Produced Sampling. At the Kalamkas field, a special scheme **(Fig. 4)** and procedure were developed to gather back-produced samples at the wellhead of polymer Injectors 20 XX, XX24, and XX41, and assess in-situ polymer mechanical degradation. The polymer injectors' geological and technical information are shown in **Table 2.** A dedicated process pipe was installed for connection to a mobile pump unit. The sampling procedure operated as follows. First, after stopping the polymer injection unit, close all valves at the wellhead. Subsequently, open the sampler to decrease pressure between the check and wing valve. Then, connect the mobile pump unit and the pressurized cylinder to the sampler. At this stage, the well is ready for backflow sampling. Furthermore, open the required valves and allow polymer backflow through the measuring tank of the mobile pump unit. Then, collect samples and change cylinders when certain volumes of polymer solution are reached. Sampling should be carried out with sufficient flushing of the cylinders (3–5 volumes of the cylinder) with the polymer solution to prevent air from entering the sample.

After collecting samples, the pressurized cylinders were immediately transported to the field laboratory to measure viscosity, using a high-precision rheometer (Anton Paar MCR 502) and aerobic conditions. Because the field laboratory does not have a glove box that provides oxygen-free conditions, polymer solutions were tested immediately (i.e., within 10–15 minutes after collection in the pressurized cylinder).
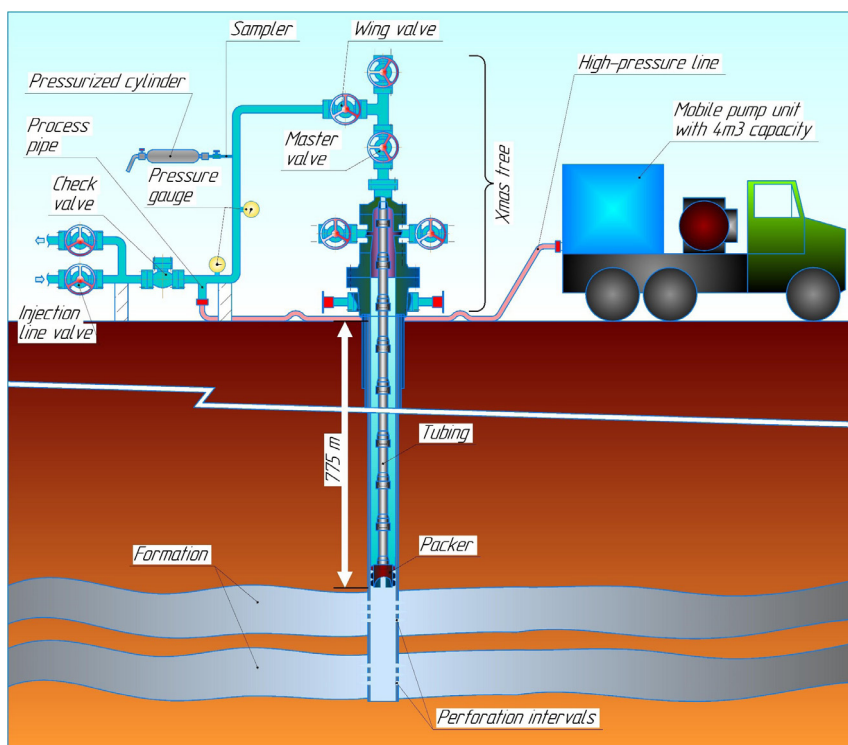
Fig. 4—Scheme to collect back-produced polymer solutions from Injector XX24.

Parameters	Well XX24	Well XX41	Well 20 XX
Tubing length [md (m)]	775	780.05	735.06
Formation top [md (m)]	780	804	795
Inner diameter of tubing (m)	0.062	0.0503	0.062
Inner diameter of casing (m)	0.14	0.0995	0.14
Perforated reservoir thickness, h (m)	10	8.5	10
Porosity, $\varnothing$ (unit fraction)	0.29	0.29	0.31
S_{wc} (unit fraction)	0.2	0.2	0.2
S_{or} (unit fraction)	0.3	0.3	0.3
w (m)	0.00381	0.00381	0.00381
V_{tubing}	2.340	1.550	2.228
V_{casing}	0.077	0.186	0.877
V_p	4	7.2	12
V_f	1.583	5.464	8.895
Deepest D_{sample}, 1 (cm)	42	84	146
Deepest D_{sample}, 2 (cm)	59	119	207
Deepest D_{sample}, 3 (cm)	2078	8436	27 422

Table 2—Wells' detailed information and the sample depth estimation for different assumptions (equations).

Measurement of viscosity of each sample should be repeated twice and averaged under conditions of minimal divergence. If the values are not similar, the measurement should be repeated. Test conditions: shear rate 7.34 s^{-1} at room temperature (~25°C). The use of a shear rate of 7.34 s^{-1} is commonly used as a standard single point for comparison of viscosities for non-Newtonian enhanced oil recovery fluids (Sheng 2011; Seright et al. 2011; Manichand et al. 2013; Seright 2017). The test temperature of ~25°C is convenient and reasonably close to the reservoir temperature (40°C). The viscosity ratio at ~25°C (room condition) to that at 40°C (reservoir condition) is roughly equal to 0.85 (i.e., if the test temperature increases from room to reservoir temperature, polymer solution viscosity simply decreases 15%). Because most liquids (including polymer solution) are incompressible at low or medium pressures, a considerable change in pressure from 14.5 to 4,350 psi causes no significant change in viscosity (Horne and Johnson 2002). Therefore, the reservoir pressure condition for polymer solution viscosity measurement is not essential.

This test procedure was carried out during planned repair work of the polymer injection unit. Consequently, the test did not affect the injection unit uptime. Also, the test has a low cost and can be done in a short time (<6 hours).

Estimated depths (D_{sample}) away from the wellbore of the collected samples were calculated based on three equations with different assumptions: Eq. 1 is based on the radial flow geometrical calculation; Eq. 2 is based on Eq. 1 and additionally considering connate water (S_{wc}) and residual oil saturation (S_{or}); Eq. 3 is based on fracture flow geometrical calculations:

$$D_{sample} = 100x \sqrt{\left(\frac{V_p - V_{tubing} - V_{casing}}{\pi \cdot h \cdot \varnothing}\right)}, \qquad (1)$$

$$D_{sample} = 100x \sqrt{\left(\frac{V_p - V_{tubing} - V_{casing}}{(1 - S_{wc} - S_{or}) \cdot \pi \cdot h \cdot \varnothing}\right)}, \qquad (2)$$

$$D_{sample} = 100x \left(\frac{V_p - V_{tubing} - V_{casing}}{2 \cdot w \cdot h}\right). \qquad (3)$$

Estimated depths for different assumptions (equations) and detailed injection wells information are shown in **Table 2.** Note that no matter which equation is applied, the calculations reveal that the back-produced volume from the injection wells was large enough to gather samples that were previously within the formation.

Polymer-solution sampling used a pressurized cylinder. The pressurized cylinders and collection procedure were specially designed for the polymer flood project to protect the solution from oxidative degradation (*API RP 63* 1990; Manichand et al. 2013). These cylinders are made of stainless steel and coated with an inert material to prevent corrosion and any iron contamination. Oxygen can be effectively excluded by carefully flushing air from the cylinder with polymer solution while collecting the sample.

Overall, the above methods, processes, and special surface equipment schemes to assess polymer solution mechanical degradation are quick, simple, cheap, and (most importantly) reliable. They were considerably easier and perhaps more reliable than those described in some other field tests (Xue et al. 2012; Morel et al. 2015; Puls et al. 2016). Based on these other field tests where substantial degradation was observed, one could argue that our methods are more reliable because they revealed only minor mechanical and/or oxidative degradation of HPAM samples and because laboratory and theoretical findings suggested that degradation should not have occurred under the conditions of the other field tests.

Field Test Results and Discussion

Injector Back-Produced Sampling. Our method for collecting back-produced HPAM solution samples was applied in three polymer injection wells: XX24, XX41, and 20 XX. The first two applications allowed us to perfect the technique, while the third (in Well 20 XX) was most successful and definitive. In each case, six to seven samples were collected as the injection well was depressurized and flowed back. The starting and ending wellhead pressures were 696 and 145 psi for Well XX24, 465 and 392 psi for Well XX41, and 640 and 162 psi for Well 20 XX, respectively. The total volumes of back-produced fluid were 4 m^3 for Well XX24, 7.2 m^3 for Well XX41, and 24 m^3 for Well 20 XX. The maximum distance of sample penetration of fluid radially into the formation (as estimated using the radial flow equation, Eq. 1) was 42 cm for Well XX24, 83.5 cm for Well XX41, and 146 cm for Well 20 XX. **Table 3** lists results for the third and most successful test (in Well 20 XX).

No. Cylinder	Back-Produced Volume at the Measuring Tank (m^3)	Estimated Location of the Collected Sample	Loss of Viscosity	Dissolved O$_2$ Concentration (ppm)
1	0	Wellhead (initial viscosity)	0%	0.2–0.3
2	8	71 cm away from the wellbore	8%	0
3	12	96 cm away from the wellbore	0%	0
4	16	115 cm away from the wellbore	0%	0
5	20	132 cm away from the wellbore	0%	0
6	24	146 cm away from the wellbore	0%	0

Table 3—Rheology measurements of the back-produced polymer solution from Injector 20 XX. The distance away from the wellbore is calculated based on Eq. 1.

For our first attempt using the procedure (in Well XX24), most of the backflowed samples contained suspended solids—apparently, because depressurization dislodged some loose sand from the formation. Viscosities on these samples were measured both before and after filtration to remove the suspended solids. Filtration caused very little reduction in viscosity, indicating that the suspended solids did not strongly affect the viscosity measurements. After filtration, the last six of the seven samples collected (representing fluid origins from 10 to 42 cm into the formation sand) experienced viscosities no lower than the injected polymer solution. The exception was that the first sample was collected after 1.2 m^3 of backflow. This sample originated from 390 m along the tubing (about the middle of the total tubing length) and exhibited 32% lower viscosity than the originally injected fluid. We suspect that this viscosity loss was due to oxidative degradation because some air leaked into the piping during the process of setting up our collection system.

In the second test (in Well XX41), the first five (of six total) back-produced polymer samples exhibited viscosity losses ranging from 50 to 75% of original viscosity. This case particularly introduced a significant amount of air while preparing for the test. Specifically, the air was introduced when the sample cylinder was (see **Fig. 4**) added/connected between the check valve and the wing valve (which required depressurization of the system). The air subsequently contributed to oxidative degradation, as seen in the first five back-produced samples. In contrast, the sixth and final sample collected (after 7.2 m^3 of flowback and originating from an estimated 83.5 cm into the formation) exhibited no viscosity loss relative to the injected polymer solution.

The test results from Wells XX24 and XX41 revealed that samples recovered relatively early in the sample-recovery process experienced some level of oxidative degradation. Therefore, we prepared a special adapter and improved our sampling method. In this improvement, this adapter was connected to the top valve **(Fig. 5),** thereby preventing oxygen from entering the pipe and wellbore space. To confirm this improvement, we measured dissolved oxygen levels throughout the testing procedure.
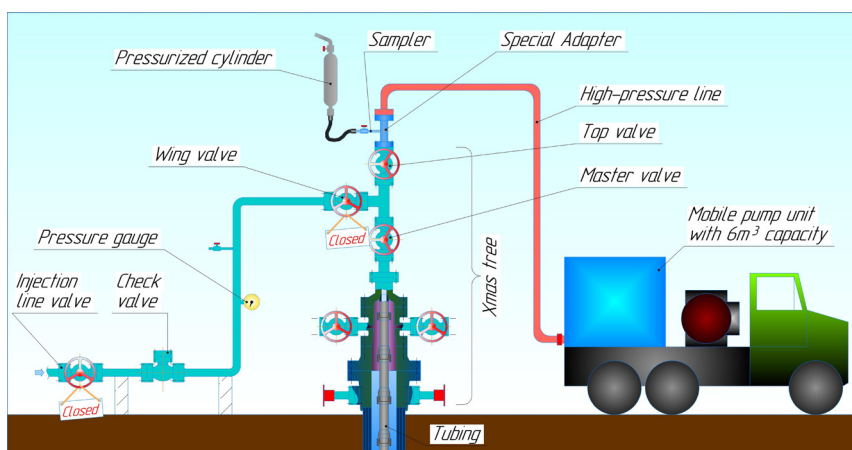
Fig. 5—The improved scheme to collect back-produced polymer solutions from Injector 20 XX.

For Well 20 XX, the planned back-produced volume was increased to 24 m^3 (three times more than previous tests). The beginning wellhead pressure was 640 psi and the test-ending pressure was 162 psi.

Back-produced sampling for Well 20 XX occurred on 24 August 2021. During the test, six samples were collected, including the first sample at the wellhead as a base sample. The typical surface temperature was 33°C during the collection.

Well 20 XX wellhead injected initial viscosity was 15.7 cp. The samples of the back-produced polymer solution **(Table 3)** did not suffer oxidative degradation, except a minor viscosity loss of 8% for Sample No. 2. This small viscosity loss may have been associated with a small amount of oxidation because of the 0.2–0.3 ppm oxygen that was injected. The first sample from the wellhead showed 0.2–0.3 ppm dissolved oxygen, and other samples from the formation contained no detectable dissolved oxygen—thus, demonstrating the effectiveness of our improved sample-collection method. Polymer solutions Sample No. 2 through Sample No. 6, which temporarily penetrated a few meters into the formation, were depleted of dissolved oxygen, even though injected solutions contained 0.2–0.3 ppm oxygen. Presumably, the 2–4% iron mineral content of the reservoir rock caused this oxygen depletion. Even though this process added

dissolved iron to the solutions, the HPAM did not degrade so long as the dissolved oxygen level remained low. To our knowledge, this is the first time that back-produced HPAM samples from an injection well have been demonstrated to contain no dissolved oxygen.

Overall, rheology measurements demonstrated the absence of polymer solution mechanical degradation during polymer injection in Wells 20 XX, XX24, and XX41.

Fig. 6 plots flux vs. distance from the wellbore dependence for Injectors 20 XX, XX24, and XX41. This calculation was based on Eq. 4 and specific conditions of the injection wells **(Table 4)**. (In this case, the flux is defined as a ratio of injection rate to radial flow filtration area.)
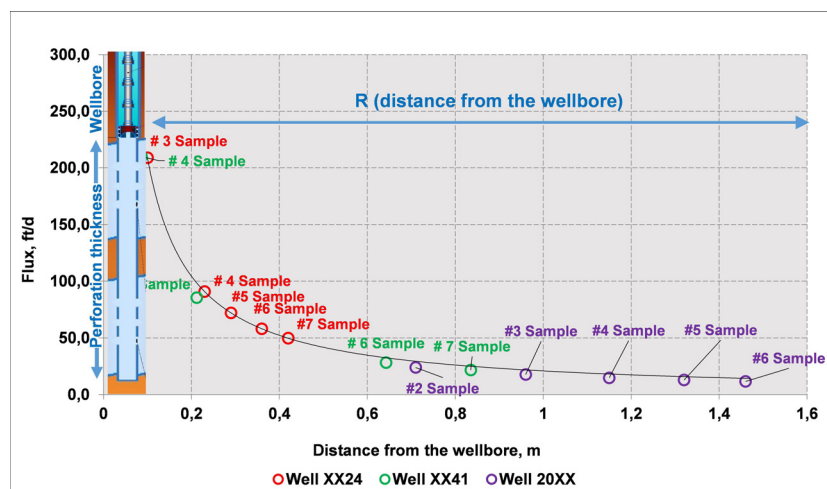
Fig. 6——Flux vs. distance from the wellbore, Well XX24 and XX41.

Parameters	Well XX24	Well XX41	Well 20 XX
Injection rate (m³/d)	400	295	326
Perforation thickness (m)	10	8.5	10
Distance from the wellbore (m)	0.10–0.42	0.086–0.835	0.71–1.46
Calculation assumptions	Openhole with no fracture present		

Table 4—Injection conditions for Wells 20 XX, XX24, and XX41.

$$\text{Flux} = 3.28084\text{x} \left(\frac{\text{Injection rate}}{2 \cdot \pi \cdot R \cdot h} \right), \tag{4}$$

where Flux = ft/D; 3.28084 = multiplier to convert meters to feet; Injection rate = m³/d; $2 \cdot \pi \cdot R \cdot h$ = the filtration area based on a radial flow, m²; R = distance from the wellbore, m; h = perforation thickness, m.

Calculations using Eq. 4 assume an openhole completion (i.e., assuming no fracture was present), so a certain distance (radius) from the wellbore corresponded to the estimated depth of collected samples (based on Eq. 1). In **Fig. 6**, Sample No. 3 for Well XX24 and Sample No. 4 for Well XX41 exhibited the highest flux (>200 ft/D). Of course, flux decreased with increased distance (radius) from the wellbore. Sample No. 6 for Well 20 XX exhibited the lowest flux (~12 ft/D). Based on our laboratory experiments in a 769-md Kalamkas reservoir core for 1,800 ppm R-1 HPAM polymer in Cretaceous formation brine (10.9% TDS), and consistent with other analog works (Maerker 1975; Seright et al. 2010), mechanical degradation occurs at a flux higher than 5 ft/D. Those results suggest that for polymer injection wells, such as 20 XX, XX24, and XX41, if injection occurs without open fractures, polymer solutions should exhibit substantial mechanical degradation. In contrast, our rheology study of formation samples revealed that the polymer solution did not exhibit mechanical degradation. This confirms that those injectors have open fractures with a high injection area that allows flux to be lower than 5 ft/D.

Producer Fluid Sampling. Many successful polymer flood projects reported that polymer eventually arrived at production wells (Zhang 1995; You et al. 2007; Wang et al. 2008a, 2008b; Moe Soe Let et al. 2012; Manichand et al. 2013). In some cases, the polymer channeled directly from an injector to a producer through a fracture (i.e., producing the same polymer concentration as injected). This circumstance occurred in one case in the Kalamkas field, where severe channeling and polymer breakthrough were observed from Injector XX37 to Producer XX87 during June 2019. Note that this polymer-channeling problem developed only once during more than 7 years of polymer injection (i.e., since 2014). The distance between the producer and injector was 400 m. After the breakthrough, polymer concentration increased from undetectable values (i.e., <1 ppm) roughly to the injected values. As will be shown later, injector pressure falloff tests after polymer injection revealed that injection occurred above the formation parting pressure and the fracture half-length was more than 300 m. This value is very close to the well spacing. Thus, in this particular case, the fracture was detrimental to sweep efficiency because it extended all the way from the injector to the producer. After several unsuccessful attempts to plug the fracture (both from the production and injection sides), the production well was shut down.

Tracer tests during water and polymer injection confirmed that the source of polymer breakthrough was Injector XX37. This unusual case provided the opportunity to collect polymer solution samples that traveled 400 m through the reservoir.

A special scheme **(Fig. 7)** and procedure were implemented to collect produced polymer solution samples at the wellhead. The sampling procedure operated as follows. First, stop Polymer Injection Well XX37 and prepare Producer Well XX87 **(Fig. 7)**. Subsequently, collect six samples at different cumulative production volumes, and then collect injecting polymer solution at Well XX37 (source of the polymer breakthrough). Proceed with viscosity measurements as described above in the subsection Injector Back-Produced Sampling and, additionally, determine the rheological power law index (*API RP 63* 1990).

Fluid sampling for Producer Well XX87 and injection of polymer solution at the wellhead of Well XX37 occurred on 30 April 2021 as described above. Samples from Producer Well XX87 were collected after polymer breakthrough and that polymer solution propagated over 400 m through the reservoir from Polymer Injection Well XX37. Additionally, the dissolved oxygen level was measured at the wellhead of Polymer Injection Well XX37 and at the last four produced samples (3, 4, 5, and 6). The viscosity and oxygen measurement results are shown in **Fig. 8** and **Table 5**. Note in **Table 5** that after the first listing (the original sample that was injected), the samples are listed in reverse chronological order of collection (i.e., Sample 6 was collected last, and Sample 1 was collected first). Test results show that injected solution from Well XX37 had roughly 1.5 ppm (i.e., between 1 and 2 ppm) dissolved oxygen content and viscosity of 25 cp with power law index of 0.763. The first three produced samples (originating closest to the surface) contained 0.2 ppm dissolved oxygen and different degrees of viscosity loss relative to the injected (25 to 50%). The last three samples show undetectable dissolved oxygen levels (less than 0.025 ppm or 25 ppb) and only modest viscosity loss (15%), with a power law index close to that of the injected solution. [We presume that the reason why significant degradation was seen for the first collected samples was that oxygen (air) was introduced into the production well during the well repair work. The gradual decrease in level of degradation (i.e., increase in viscosity) with time reflected flushing this oxygen out of the system.] These findings indicate that injected oxygen in the polymer solution (that transported 400 m through the Kalamkas reservoir) was consumed by the surrounding reservoir rock and provided chemical (oxidative) stability of the solution (due to iron-containing minerals up to 2 to 4%; Seright et al. 2011). This small viscosity loss (from 25 to 21 cp) was probably associated with oxidative viscosity decrease in the wellbore of Polymer Injection Well XX37. (Viscosity was measured at the wellhead, then solution passed through the tubing approximately 30 minutes before entering the formation. This time was sufficient to degrade the solution viscosity by 15%.)
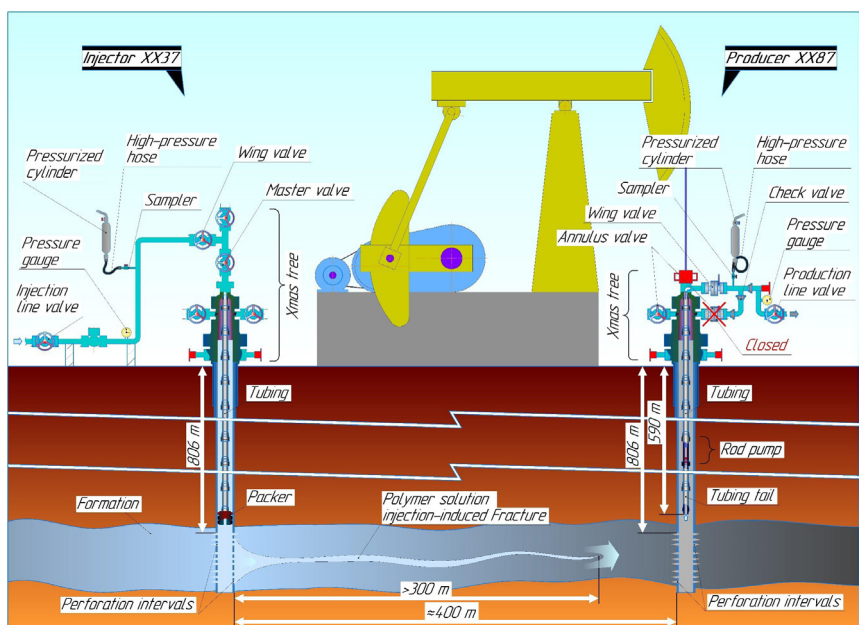
Fig. 7—Scheme to collect polymer solutions from Producer Well XX87.
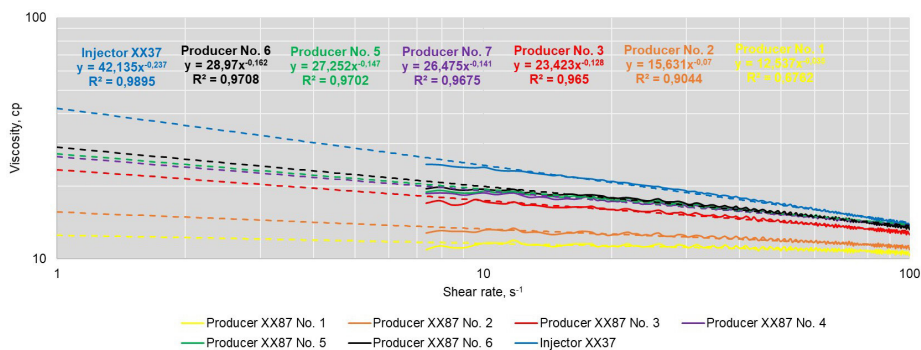
Fig. 8—Rheological curve analysis of injected (Well XX37) and produced (Well XX87) polymer solutions.

Well	Produced Volume (m³)	Dissolved O₂ Concentration (ppm)	Location of the Collected Sample	Viscosity at 7.34 s⁻¹ (cp)	Power Law Index n (imensionless)[1]
Injector XX37		≈1.5 (>1 and <2)	Injected	25.1	1−0.237 = 0.763
Producer XX87 No. 6	6.5	0	Formation	21.0	1−0.162 = 0.838
Producer XX87 No. 5	4.4	0	Between tubing and perforation	21.3	1−0.147 = 0.853
Producer XX87 No. 4	3.6	0	Between tubing and perforation	21.3	1−0.141 = 0.859
Producer XX87 No. 3	3.3	0.2	Between tubing and perforation	19.2	1−0.128 = 0.872
Producer XX87 No. 2	2.9	N/A	Between tubing and perforation	14.9	1−0.070 = 0.930
Producer XX87 No. 1	2.0	N/A	Downhole tubing	13.1	1−0.035 = 0.965

[1](API RP 63 1990)

Table 5—Rheology measurements of the injected and produced polymer solutions from Injector XX37 and Producer XX87.

Pressure Falloff Tests. To obtain valuable well test data, we ran pressure falloff tests in injection wells. These tests were performed during polymer injection for Wells XX24, XX41, 20 XX, and XX37 in 2020 and during the waterflood in 2019, except Wells 20 XX and XX37 (well tests not conducted). For Wells XX24 and XX41, two combined pressure transient analyses are presented in **Figs. 9 and 10,** and their interpretations are in **Tables 6 and 7.** For Well XX37, pressure falloff test analysis during polymer injection is presented in **Fig. 11** and **Table 8.** For Well 20 XX, pressure falloff test analysis during polymer injection is presented in **Fig. 12** and **Table 9.** The pressure transient analysis includes plotting pressure vs. time and the Bourdet derivative on a log-log scale (based on Houze et al. 2020). Comparison and analysis of two pressure curves (original and derivative) for each flood can reveal signatures of numerous well, reservoir, and boundary behaviors. In our case, the analyses of pressure falloff tests indicated the absence of fractures during waterflood (green curves), but during the polymer flood (red curves), injection occurred above the formation parting pressure. The fracture half-lengths for Wells 20 XX, XX24, and XX41 were pproximately 100 m. For Well XX37, where severe channeling and polymer breakthrough was observed, fracture half-length was close to the well spacing. We can see that polymer injection leads to well stimulation and as a consequence, the polymer solution flows through the perforations and near-wellbore zone with an area high enough to ensure mechanical stability of the solution. If Wells 20 XX, XX24, XX41, and XX37 were not fractured, injection of viscous polymer solution would necessarily decrease injectivity, roughly in
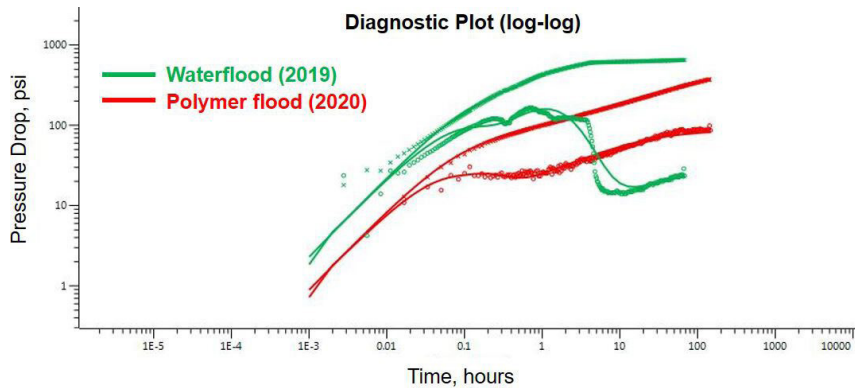
Fig. 9—Analysis of pressure falloff tests during water and polymer injection into Well XX24.
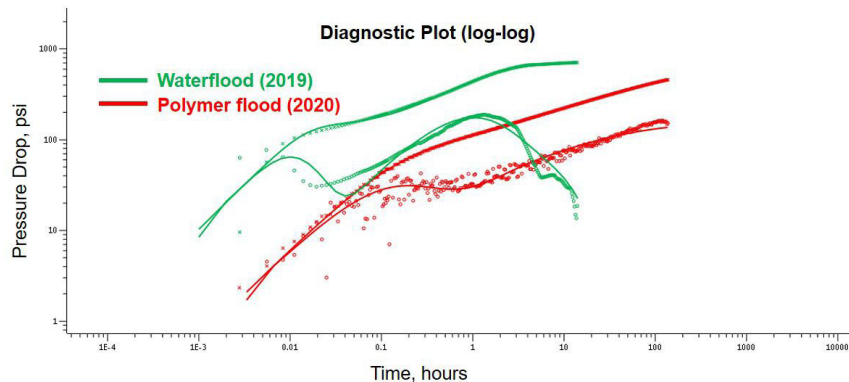
Fig. 10—Analysis of pressure falloff tests during water and polymer injection into Well XX41.

No.	Parameter	Value During Waterflood (2019)	Value During Polymer Flood (2020)
1	Perforation interval (top-bottom)	780–805 m	780–805 m
2	Test duration (hours)	69.2	146
3	Wellbore storage (WBS) model	Changing WBS	Changing WBS
4	Well model	Vertical	Vertical fractured finite conductivity
5	Reservoir model	Homogenous	Homogenous
6	Boundary model	One fault	Infinite
7	Reservoir pressure (psi)	1,075	1,270
8	Conductivity (md·m)	3 764	8 596
9	Average permeability (md)	362	860
10	Total skin	13.4	−5.8
11	Geometrical skin	-	−6.1
12	Fracture half-length (m)	-	101.0
13	Fracture conductivity (md·m)	-	7.93E + 6
14	Fracture permeability (md)	-	39 292
15	Injectivity index [bbl/(d·psi)]	3.17	6.62

Table 6—Analysis of pressure falloff tests during water and polymer injection into Well XX24.

proportion to the polymer solution viscosity (Seright et al. 2009; Manichand et al. 2013). In our case, the expected injectivity without open fractures would be 16 times lower than that for water, but in fact, our injectivity was enhanced by a factor from 1.3 to 2.1 **(Tables 6–9)**.

Step-Rate Tests. To evaluate and confirm obtained results from pressure falloff tests, we ran step-rate tests in water and polymer injection wells. These tests were performed at Polymer Injectors XX24 and XX41, and at Water Injector XX47, which is an offset well for polymer injectors, so it has the same reservoir characteristics (formation height, layering, and permeability) and technical conditions (perforation intervals, injection rate, number of surrounded production wells, voidage replacement ratio, and well spacing). **Fig. 13** plots injection rate vs. pressure drop for Wells XX24, XX41, and XX47. Results of step-rate tests and analysis are in **Table 10.**

The step-rate test was performed as follows. First, the injector current operating flow rate and wellhead pressure were measured. Next, we decreased the injection rate to the next step and allowed pressures to stabilize, and wellhead pressure was determined again. This process was repeated in stages to determine the wellhead pressures at lower flow rates. Then we converted wellhead pressures to the well flowing BHPs and the reservoir pressure was determined by extrapolating the inflow performance relationship (IPR) curve to zero flow rate. Finally, we plotted flow rate and pressure drop associated with solid circles for Water Injector XX47, solid triangles for Polymer Injector XX41, and solid squares for Polymer Injector XX24. The resulting dashed lines are IPRs, and their slopes (a multiplier of "x" variable in the linear equation) are injectivity indexes. For the water injector, the flow rate was controlled by the choke. In contrast, for the polymer injector, flow rate control was achieved by reducing the engine speed of individual plunger pumps. A flow rate of 144 m^3/d was the lowest operating rate and 400 m^3/d was the highest technical flow rate for an individual plunger pump within the polymer injection system.

No.	Parameter	Value During Waterflood (2019)	Value During Polymer Flood (2020)
1	Perforation interval (top-bottom)	804–807, 810–812, 813.5–817 m	804–807, 810–812, 813.5–817 m
2	Test duration (hours)	71.8	140.9
3	Wellbore storage (WBS) model	Changing WBS	Changing WBS
4	Well model	Vertical	Vertical fractured finite conductivity
5	Reservoir model	Homogenous	Homogenous
6	Boundary model	Circle (ReP-const)	Infinite
7	BHP (psi)	1,822	1,874
8	Conductivity (md·m)	972	3 604
9	Average permeability (md)	135	424
10	Total skin	1.46	−5.9
11	Geometrical skin	-	−6.0
12	Fracture half-length (m)	-	102.3
13	Fracture conductivity (md·m)	-	4.45E + 6
14	Fracture permeability (md)	-	2 174
15	Injectivity index [bbl/(d·psi)]	2.08	3.77

Table 7—Analysis of pressure falloff tests during water and polymer injection into Well XX41.

Diagnostic Plot (log-log)
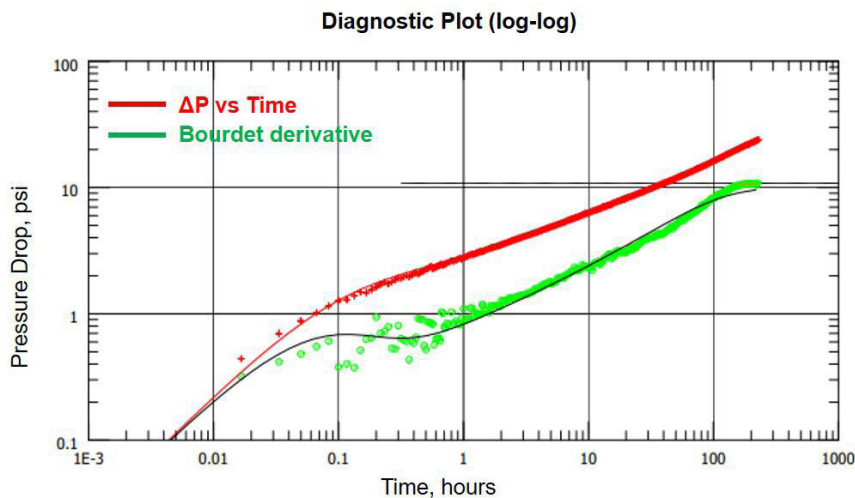
Fig. 11—Analysis of pressure falloff test during polymer injection into Well XX37.

| | | Value | |
No.	Parameter	During Polymer Flood (2020)	During Waterflood (2018)
1	Perforation interval (top-bottom)	806–810, 812.5–820.5 m	806–810, 812.5–820.5 m
2	Test duration (hours)	233.6	N/A
3	Wellbore storage (WBS) model	Changing WBS	
4	Well model	Vertical fractured finite conductivity	
5	Reservoir model	Homogenous	
6	Boundary model	Infinite	
7	Reservoir pressure (psi)	1,252	
8	Conductivity (md·m)	5 630	
9	Average permeability (md)	503.1	
10	Total skin	−7.13	
11	Geometrical skin	0.1	
12	Fracture half-length (m)	308	
13	Fracture conductivity (md·m)	0.384E + 6	
14	Fracture permeability (md)	623	
15	Injectivity index [bbl/(d·psi)]	2.47	1.86

Table 8—Analysis of pressure falloff test during polymer injection into Well XX37.

Diagnostic Plot (log-log)
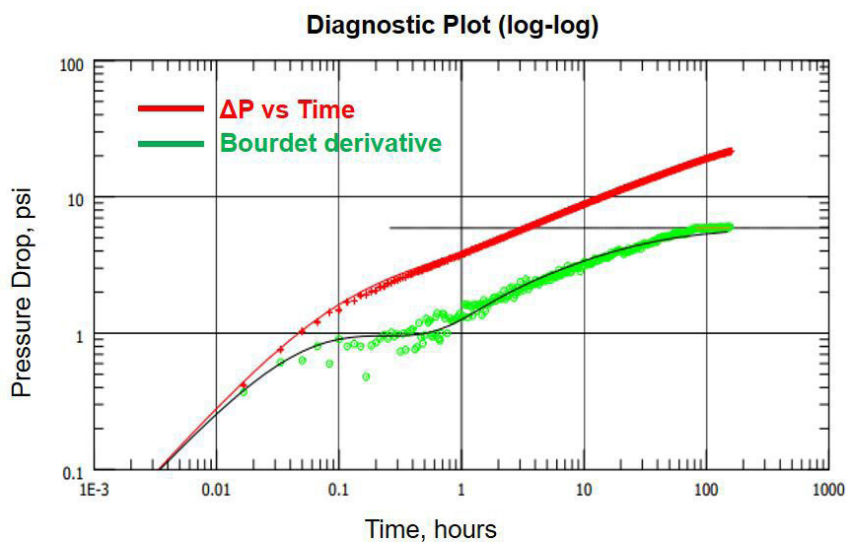
Fig. 12—Analysis of pressure falloff test during polymer injection into Well 20 XX.

No.	Parameter	Value	
		During Polymer Flood (2020)	During Waterflood (2014)
1	Perforation interval (top-bottom)	795–826 m	795–826 m
2	Test duration (hours)	163.5	N/A
3	Well model	Vertical fractured finite conductivity	
4	Reservoir model	Homogenous	
5	Boundary model	Infinite	
6	Reservoir pressure (psi)	1,099	
7	BHP (psi)	1,794	
8	Conductivity (md·m)	1 260	
9	Average permeability (md)	440.5	
10	Total skin	−6.16	
11	Geometrical skin	0.12	
12	Fracture half-length (m)	116	
13	Fracture conductivity (md·m)	0.1E + 6	
14	Injectivity index [bbl/(d·psi)]	3.86	2.21

Table 9—Analysis of pressure falloff test during polymer injection into Well 20 XX.
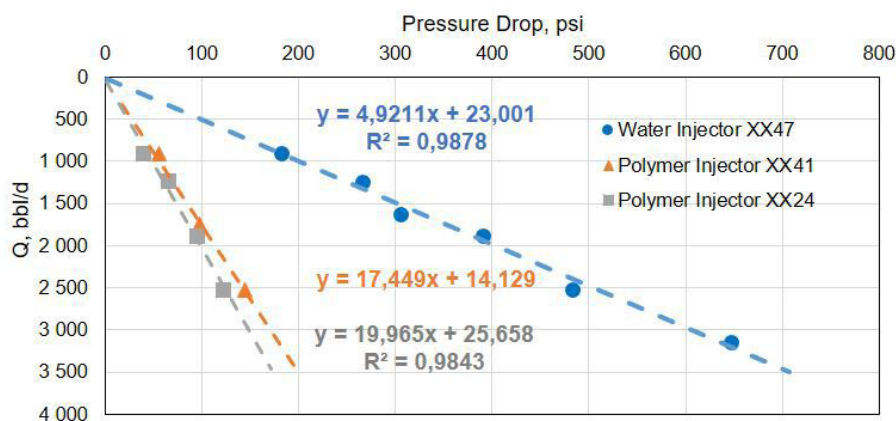
Fig. 13—Analysis of pressure step-rate tests during water and polymer injection into Wells XX47, XX24, and XX41.

Step No.	Injection Rate (B/D)	Water Injector XX47			Polymer Injector XX24			Polymer Injector XX41		
		Pwellhead (psi)	BHP (psi)	dP (psi)	Pwellhead (psi)	BHP (psi)	dP (psi)	Pwellhead (psi)	BHP (psi)	dP (psi)
1	906	319	1,625	182	653	1,851	40	544	1,773	56
2	1,238	406	1,709	266	682	1,877	66	557	1,783	66
3	1,630	450	1,749	306						
4	1,751							595	1,815	98
5	1,887	537	1,833	390	718	1,907	95			
6	2,521	638	1,926	483	740	1,933	122	638	1,862	145
7	3,140	812	2,090	647						
Reservoir pressure (psi)		1,443			1,811			1,717		
Injectivity [bbl/(d·psi)]		4.9			20.0			17.4		

Table 10—Analysis of pressure step-rate tests during water and polymer injection into Wells XX47, XX24, and XX41.

Comparison and analysis of IPRs during water and polymer injection confirm pressure falloff test analysis that the injectivity index during polymer injection was much higher than during waterflood. The step-rate test showed enhanced injectivity during the polymer flood relative to waterflooding (i.e., roughly four times greater than expected). Previous work has shown that viscoelastic (or shear thickening) behavior of HPAM polymers occurs at high fluxes, and as a consequence induces a fracture to form and extend in the well (Ma and McClure 2016).

The presence of fractures during the polymer flood is consistent with the fact that most of the worldwide polymer flood projects inject into vertical wells above the formation parting pressure (Seright et al. 2009; Van den Hoek et al. 2009, Van den Hoek et al. 2012; Seright 2017), where linear flow is expected. In contrast, if fractures or fracture-like features are not present during polymer injection, achieving a favorable economical injection rate and acceptable voidage replacement ratio (e.g., the same as during a waterflood) is not practical. Additionally, according to the analytical calculations of Seright (2017) and the work of Dyes et al. (1958), fractures may not seriously

affect a sweep efficiency if the fracture half-length is less than one-third of the well spacing. These findings reveal that the advantages of fracture features during polymer flooding (i.e., little or no injectivity loss and mechanical stability of the polymer solution) outweigh its disadvantages (e.g., possible severe channeling and jeopardized sweep efficiency).

Rheology in Porous Media and Mechanical Degradation. The purpose of this section is to demonstrate (using laboratory measurements) that severe mechanical degradation would have been observed during HPAM injection of our wells if fractures or fracture-like features were not present. Rheology in porous media and mechanical degradation is directly related to the fluid velocity or flux in porous media (Maerker 1975; Seright et al. 2009, Seright et al. 2011; Manichand et al. 2013). Consequently, using the methods described in Seright et al. (2011), we determined rheology in a 769-md Kalamkas reservoir core for 1800-ppm R-1 HPAM polymer in Cretaceous formation brine (10.9% TDS). **Fig. 14** plots resistance factor vs. flux for this solution. (Resistance factor is the effective viscosity in porous media relative to water.) **Fig. 15** plots viscosity (measured at 7.34 s^{-1} and 25°C, and expressed as a percentage of the injected polymer solution viscosity) for the effluent vs. flux at which the polymer solution was forced through the core. **Fig. 16** plots fresh polymer solution viscosity vs. shear rate before injecting in the reservoir core.

Fig. 14 was generated as follows. First, we performed standard core analysis to determine porosity and permeability. Next, the core was saturated with Kalamkas Cretaceous formation brine and permeability was determined. Subsequently, we injected freshly prepared 1,800-ppm R-1 HPAM (in the Kalamkas Cretaceous formation brine) at moderate flux (50 ft/D) and measured the stabilized resistance factor. Then we decreased flux to 30 ft/D and allowed pressures to stabilize and resistance factor to be determined again. This process was repeated in stages to determine the resistance factors associated with the solid squares in **Fig. 14.** The dashed curve in **Fig. 14** shows viscosity vs. flux which corresponds to the calculated shear rate using the model described in Hirasaki and Pope (1974). Between 50 and 11 ft/D, the resistance factor appeared to be constant with decreasing flux. As flux was lowered from 11 to 1 ft/D, the resistance factor decreased dramatically with decreasing flux. The literature has reported this behavior (Maerker 1975; Seright et al. 2011) as a shear thickening or dilatant or viscoelastic effect. Shear thickening in porous media has been attributed to increased stresses and energy expenditure associated with disentanglement and elongation of coiled HPAM molecules as they flow through the sequentially contracting/dilating flow paths within porous media. For each flux between 50 and 5.2 ft/D, the polymer was mechanically degraded to a different extent, as demonstrated by the solid squares in **Fig. 15**.

For flux values lower than 1 ft/D, a modest shear thinning was seen, as resistance factor increased with decreasing flux **(Fig. 14)** and no mechanical degradation occurred. Furthermore, this resistance factor increase correlated reasonably well with the polymer viscosity increase as shear rate (or flux) decreased.

Recall from **Fig. 6** that the Darcy velocity (flux) at the injection sandface for an openhole completion would be over 200 ft/D. Thus, from **Fig. 14,** the anticipated mechanical degradation would have been over 70% if the completion was the open hole with no fracture
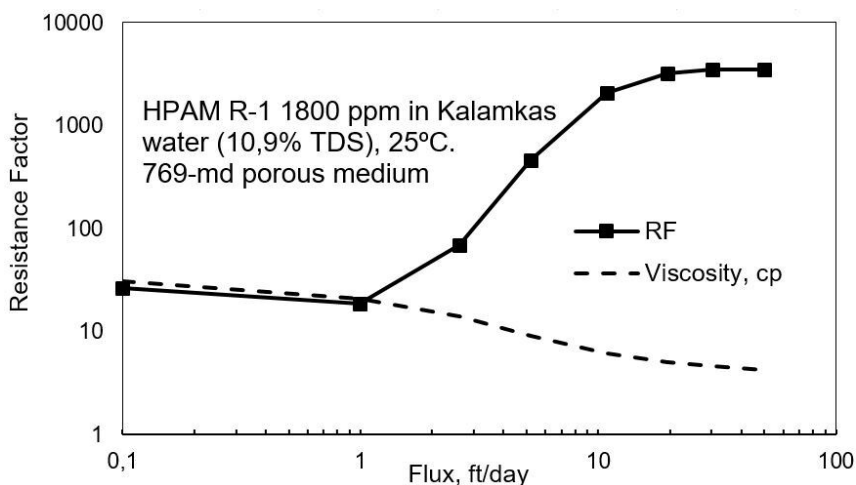
Fig. 14—Resistance factor vs. flux for R-1 HPAM in the Kalamkas water.
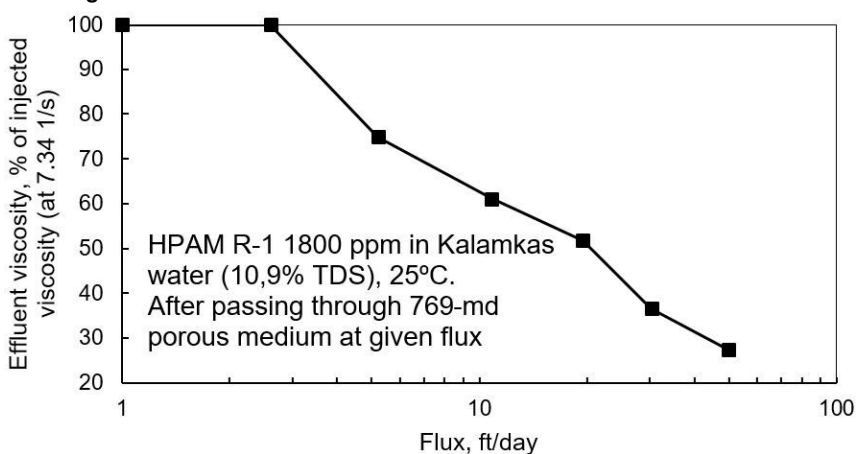
Fig. 15—Viscosities of solutions after being forced through the core at a given flux.
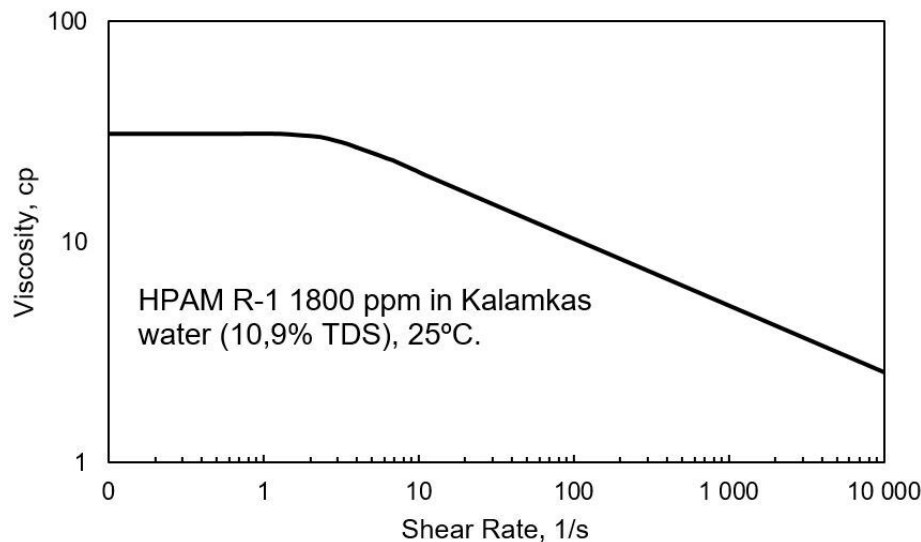
Fig. 16—Viscosity vs. shear rate for 1,800 ppm R-1 HPAM in the Kalamkas water.

present. Therefore, the presence of the open fracture provides the logical explanation for both the observed lack of severe degradation and lack of severe injectivity loss for the HPAM injection well.

Significance of the Results. As mentioned earlier, the very large investment associated with the polymer bank during a polymer flood necessitates a determination that the polymer is not substantially degraded during the process of injection. This paper provides a new methodology that is much more cost-effective for assessing near-wellbore polymer degradation than in previous methods, and the methodology is demonstrated for an important field application in Kazakhstan. In addition, this paper provides field-based support that vertical polymer injection wells have open fractures that enhance injectivity. We especially demonstrate that these fractures reduce polymer mechanical degradation to a level that mitigates this degradation concern in a field setting.

Conclusions

The goal of this paper was to demonstrate certain predictions about the existence and effects of fractures on injectivity during injection of HPAM solutions into vertical wells during a polymer flood in the Kalamkas field in Western Kazakhstan. As detailed in the section Novelty and Expected Value from the Current Work, this paper provides field evidence to clarify the utility of near-wellbore fractures to promote injectivity and mitigate mechanical degradation of HPAM solutions. It also provides a sampling methodology that demonstrated minimum mechanical and oxidative degradation under field circumstances, whereas previous sampling methods may have provided overly pessimistic indications of HPAM stability. The following findings were noted:

1. Step-rate tests indicated that fractures were not open during water injection before polymer injection. In contrast, during polymer injection, open fractures were confirmed using step-rate tests, pressure transient analysis, and comparison of actual injectivities vs. those calculated using the Darcy radial flow equation coupled with laboratory measurements of HPAM rheology in Kalamkas cores.
2. We developed a novel method to assess in-situ polymer solution mechanical stability during a polymer flood. Under Kalamkas field conditions, we demonstrated the collection of formation samples using the natural energy of a reservoir at the wellhead. This process protected polymer solution samples from oxidative degradation. Compared to other laboratory and field methods, this novel method is quick, simple, and inexpensive. Compared with other field tests where substantial degradation was observed, one could argue that our methods are more reliable because they revealed only minor mechanical and/or oxidative degradation of HPAM samples and because laboratory and theoretical findings suggested that degradation should not have occurred under the conditions of the other field tests.
3. Rheology measurements of back-produced polymer solutions showed the absence of the mechanical degradation. This finding provided further confirmation that polymer injection occurred above the formation parting pressure and that the injection area associated with the fracture was large enough to ensure the stability of the solution.
4. These findings confirm that the advantages of fractures or fracture-like features during a polymer flood (i.e., little or no injectivity loss; mechanical stability of the polymer solution) can outweigh their disadvantages (e.g., possible severe channeling and jeopardized sweep efficiency).
5. Polymer solutions that were back-produced from injection wells were depleted of dissolved oxygen, even though injected solutions contained 200–300 ppb of dissolved oxygen and the polymer solutions only penetrated a few meters into the formation. Presumably, the 2–4% iron mineral content of the reservoir rock caused this oxygen depletion. Even though this process added dissolved iron to the solutions, the HPAM did not degrade so long as the dissolved oxygen level remained low.
6. Polymer solutions that propagated over 400 m through a fracture from an injector to a producer were also depleted of dissolved oxygen, but suffered only minor viscosity loss (15%) after traveling all the way through the formation.

The significance and novelty of the last four conclusions may be appreciated by realizing that virtually all previous field tests (where produced samples were analyzed from production wells or back-produced samples were analyzed from injection wells) indicated substantial HPAM degradation (as revealed in our literature review). If accepted at face value, those previous results would cast serious doubt on the viability of all HPAM floods. In contrast, our results alleviate those doubts by demonstrating that HPAM stability in a field application is consistent with present and previous laboratory and theoretical expectations. Our results suggest that the lack of stability observed in the previous tests may have been due to problems with the sampling procedures—rather than degradation that jeopardized the polymer in the reservoir.

Nomenclature

D_{sample} = formation sample depth, cm
h = perforation thickness, m
S_{or} = residual oil saturation, unit fraction
S_{wc} = connate water saturation, unit fraction
V_{casing} = volume between tubing end and perforation bottom, m^3
V_f = volume back-produced from formation, m^3
V_p = back-produced volume, m^3
V_{tubing} = tubing inner volume, m^3
w = fracture width, m
$ø$ = porosity, unit fraction

Acknowledgments

References

API RP 63, *Recommended Practices for Evaluation of Polymers Used in Enhanced Oil Recovery Operations*. 1990. Washington, DC: American Petroleum Institute.

Åsen, S. M., Stavland, A., and Strand, D. 2019. An Experimental Investigation of Polymer Mechanical Degradation at the Centimeter and Meter Scale. *SPE J.* **24** (4): 1700–1713. SPE-190225-PA. https://doi.org/10.2118/190225-PA.

Dandekar, A., Bai, B., and Barnes, J. 2019. First Ever Polymer Flood Field Pilot - A Game Changer to Enhance the Recovery of Heavy Oils on Alaska's North Slope. Paper presented at the SPE Western Regional Meeting, San Jose, California, USA, 23–26 April. SPE-195257-MS. https://doi.org/10.2118/195257-MS.

Dauben, D. L. and Menzie, D. E. 1967. Flow of Polymer Solutions Through Porous Media. *J Pet Technol* **19** (8): 1065–1073. SPE-1688-PA. https://doi.org/10.2118/1688-PA.

Delamaide, E. 2019. How to Use Analytical Tools to Forecast Injectivity in Polymer Floods. Paper presented at the SPE Europec Featured at 81st EAGE Conference and Exhibition, London, England, UK, 3–6 June. SPE-195513-MS. https://doi.org/10.2118/195513-MS.

Dyes, A. B., Kemp, C. E., and Caudle, B. H. 1958. Effect of Fractures on Sweep-out Pattern. *Trans* **213** (1): 245–249. SPE-1071-G. https://doi.org/10.2118/1071-G.

Garrepally, S., Jouenne, S., and Leuqeux, F. 2020. Polymer Flooding - Towards a Better Control of Polymer Mechanical Degradation at the Near Wellbore. Paper presented at the SPE Improved Oil Recovery Conference, Virtual, August 31–September 4. SPE-200373-MS. https://doi.org/10.2118/200373-MS.

Heemskerk, J., Rosmalen, R., and Janssen-van, R. 1984. Quantification of Viscoelastic Effects of Polyacrylamide Solutions. Paper presented at the SPE Enhanced Oil Recovery Symposium, Tulsa, Oklahoma, USA, 15–18 April. SPE-12652-MS. https://doi.org/10.2118/12652-MS.

Hirasaki, G. J. and Pope, G. A. 1974. Analysis of Factors Influencing Mobility and Adsorption in the Flow of Polymer Solution Through Porous Media. *SPE J.* **14** (4): 337–346. SPE-4026-PA. https://doi.org/10.2118/4026-PA.

Horne, R. A. and Johnson, D. S. 2002. The Viscosity of Water Under Pressure. *J Phys Chem* **70** (7): 2182–2190. https://doi.org/10.1021/j100879a018.

Houze, O., Viturat, D., Fjaere, O. S. et al. 2020. *Dynamic Data Analysis* v5.30.01. Turin, Italy: KAPPA.

Jouenne, S., Chakibi, H., and Levitt, D. 2017. Polymer Stability After Successive Mechanical-Degradation Events. *SPE J.* **23** (1): 18–33. SPE-186103-PA. https://doi.org/10.2118/186103-PA.

Lake, L. W. 1989. *Enhanced Oil Recovery*. Enlglewood Cliffs, New Jersey, USA: Prentice Hall.

Leibin, E. L. and Ogay, E. K. 1979. Technological Scheme of the Kalamkas Field Development. KazNIPIneft report. Shevchenko (in Russian).

Lotfollahi, M., Farajzadeh, R., and Delshad, M. 2016. Mechanistic Simulation of Polymer Injectivity in Field Tests. *SPE J.* **21** (4): 1178–1191. SPE-174665-PA. https://doi.org/10.2118/174665-PA.

Ma, Y. and McClure, M. W. 2016. The Effect of Polymer Rheology and Induced Fracturing on Injectivity and Pressure-Transient Behavior. *SPE Res Eval & Eng* **20** (2): 394–402. SPE-184389-PA. https://doi.org/10.2118/184389-PA.

Maerker, J. M. 1975. Shear Degradation of Partially Hydrolyzed Polyacrylamide Solutions. *SPE J.* **15** (4): 311–322. SPE-5101-PA. https://doi.org/10.2118/5101-PA.

Manichand, R. N., Moe Soe Let, K. P., and Gil, L. 2013. Effective Propagation of HPAM Solutions through the Tambaredjo Reservoir during a Polymer Flood. *SPE Prod & Oper* **28** (4): 358–368. SPE-164121-PA. https://doi.org/10.2118/164121-PA.

Moe Soe Let, K. P., Manichand, R. N., and Seright, R. S. 2012. Polymer Flooding a ~500-Cp Oil. Paper presented at the Eighteenth SPE Improved Oil Recovery Symposium, Tulsa, Oklahoma, USA, 14–18 April. SPE-154567-MS. https://doi.org/10.2118/154567-MS.

Moradi-Araghi, A. and Doe, P. H. 1987. Hydrolysis and Precipitation of Polyacrylamides in Hard Brines at Elevated Temperatures. *SPE Res Eng* **2** (2): 189–198. SPE-13033-PA. https://doi.org/10.2118/13033-PA.

Morel, D. C., Zaugg, E., and Jouenne, S. 2015. Dalia/Camelia Polymer Injection in Deep Offshore Field Angola Learnings and In Situ Polymer Sampling Results. Paper presented at the SPE Asia Pacific Enhanced Oil Recovery Conference, Kuala Lumpur, Malaysia, 11–13 August. SPE-174699-MS. https://doi.org/10.2118/174699-MS.

Morris, C. W. and Jackson, K. M. 1978. Mechanical Degradation Of Polyacrylamide Solutions In Porous Media. Paper presented at the SPE Symposium on Improved Methods of Oil Recovery, Tulsa, Oklahoma, USA, 16–17 April. SPE-7064-MS. https://doi.org/10.2118/7064-MS.

Noïk, Ch., Delaplace, Ph., and Muller, G. 1995. Physico-Chemical Characteristics of Polyacrylamide Solutions after Mechanical Degradation through a Porous Medium. Paper presented at the SPE International Symposium on Oilfield Chemistry, San Antonio, Texas, USA, 14–17 February. SPE-28954-MS. https://doi.org/10.2118/28954-MS.

Puls, C., Clemens, T., and Sledz, C. 2016. Mechanical Degradation of Polymers During Injection, Reservoir Propagation and Production - Field Test Results 8 TH Reservoir, Austria. Paper presented at the SPE Europec Featured at 78th EAGE Conference and Exhibition, Vienna, Austria, 30 May–2 June. SPE-180144-MS. https://doi.org/10.2118/180144-MS.

Putz, A. G., Bazin, B., and Pedron, B. M. 2013. Commercial Polymer Injection in the Courtenay Field, 1994 Update. Paper presented at the SPE Annual Technical Conference and Exhibition, New Orleans, Louisiana, USA, 25–28 September. SPE-28601-MS. https://doi.org/10.2118/28601-MS.

Seright, R. S. 1983. The Effects of Mechanical Degradation and Viscoelastic Behavior on Injectivity of Polyacrylamide Solutions. *SPE J.* **23** (3): 475–485. SPE-9297-PA. https://doi.org/10.2118/9297-PA.

Seright, R. S. 2017. How Much Polymer Should Be Injected During a Polymer Flood? Review of Previous and Current Practices. *SPE J.* **22** (1): 1–18. SPE-179543-PA. https://doi.org/10.2118/179543-PA.

Seright, R. S., Campbell, A. R., and Mozley, P. S. 2010. Stability of Partially Hydrolyzed Polyacrylamides at Elevated Temperatures in the Absence of Divalent Cations. *SPE J.* **15** (2): 341–348. SPE-121460-PA. https://doi.org/10.2118/121460-PA.

Sagyndikov, M., Mukhambetov, B., Orynbasar, Y. et al. 2018. Evaluation of Polymer Flooding Efficiency at Brownfield Development Stage of Giant Kalamkas Oilfield, Western Kazakhstan. Paper presented at the SPE Annual Caspian Technical Conference and Exhibition, Astana, Kazakhstan, 31 October–2 November. SPE-192555-MS. https://doi.org/10.2118/192555-MS.

Seright, R. and Brattekas, B. 2021. Water Shutoff and Conformance Improvement: An Introduction. *Pet Sci* **18** (2): 450–478. https://doi.org/10.1007/s12182-021-00546-1.

Seright, R. S., Fan, T., and Wavrik, K. 2011. New Insights into Polymer Rheology in Porous Media. *SPE J.* **16** (1): 35–42. SPE-129200-PA. https://doi.org/10.2118/129200-PA.

Seright, R. S., Seheult, J. M., and Talashek, T. A. 2009. Injectivity Characteristics of EOR Polymers. *SPE Res Eval & Eng* **12** (5): 783–792. SPE-115142-PA. https://doi.org/10.2118/115142-PA.

Seright, R. S. and Skjevrak, I. 2015. Effect of Dissolved Iron and Oxygen on Stability of Hydrolyzed Polyacrylamide Polymers. *SPE J.* **20** (3): 433–441. SPE-169030-PA. https://doi.org/ doi:10.2118/169030-PA.

Seright, R. S., Wavrik, K. E., Zhang, G. et al. 2021. Stability and Behavior in Carbonate Cores for New Enhanced-Oil-Recovery Polymers at Elevated Temperatures in Hard Saline Brines. *SPE Res Eval & Eng* **24** (1): 1–18. SPE-200324-PA. https://doi.org/10.2118/200324-PA.

Shao, Z. B., Zhou, J. S., and Sung, G. 2005. Studies on Mechanical Degradation of Partially Hydrolyzed Polyacrylamide in Course of Polymer Flooding: Changes in Relative Molecular Mass, Viscosity and Related Parameters. *Oilfield Chemistry* **22** (1): 72–77.

Sheng, J. 2011. *Modern Chemical Enhanced Oil Recovery: Theory and Practice, Chapter 5-Polymer Flooding*. Amsterdam: Elsevier.

Shupe, R. D. 1981. Chemical Stability of Polyacrylamide Polymers. *J Pet Technol* **33** (8): 1513–1529. SPE-9299-PA. https://doi.org/10.2118/9299-PA.

Skauge, T., Skauge, A., and Salmo, I. C. 2016. Radial and Linear Polymer Flow - Influence on Injectivity. Paper presented at the SPE Improved Oil Recovery Conference, Tulsa, Oklahoma, USA, 11–13 April. SPE-179694-MS. https://doi.org/10.2118/179694-MS.

Sulin, V. A. 1946. *Waters of Petroleum Formations in the System of Nature Waters*, 96. Moscow: Gostoptekhizdat.

Tai, I., Giddins, M. A., and Muggeridge, A. 2021. Improved Calculation of Wellblock Pressures for Numerical Simulation of Non-Newtonian Polymer Injection. *SPE J.* **26** (4): 2352–2363. SPE-205339-PA. https://doi.org/10.2118/205339-PA.

Van den Hoek, P., Al-Masfry, R. A., and Zwarts, D. 2009. Optimizing Recovery for Waterflooding under Dynamic Induced Fracturing Conditions. *SPE Res Eval & Eng* **12** (5): 671–682. SPE-110379-PA. https://doi.org/10.2118/110379-PA.

Van den Hoek, P. J., Mahani, H., and Sorop, T. G. 2012. Application of Injection Fall-Off Analysis in Polymer Flooding. Paper presented at the SPE Europec/EAGE Annual Conference, Copenhagen, Denmark, 4–7 June. SPE-154376-MS. https://doi.org/10.2118/154376-MS.

Wang, D., Han, P., and Shao, Z. 2008a. Sweep-Improvement Options for the Daqing Oil Field. *SPE Res Eval & Eng* **11** (1): 18–26. SPE-99441-PA. https://doi.org/10.2118/99441-PA.

Wang, D., Seright, R. S., and Shao, Z. 2008b. Key Aspects of Project Design for Polymer Flooding at the Daqing Oilfield. *SPE Res Eval & Eng* **11** (6): 1117–1124. SPE-109682-PA. https://doi.org/10.2118/109682-PA.

Xue, X., Han, M., Zhang, L. et al. 2012. The Down Hole Sampling Investigation of Polymer Solutions in Bohai Oilfield. *China Offshore Oil and Gas J* **24** (5): 37–39.

Yang, S. H. and Treiber, L. E. 2013. Chemical Stability of Polyacrylamide Under Simulated Field Conditions. Paper presented at the SPE Annual Technical Conference and Exhibition, Las Vegas, Nevada, 22–26 September. SPE-14232-MS. https://doi.org/10.2118/14232-MS.

You, Q., Wang, F. L., and Mu, L. N. 2007. Comparison of the Properties of Injected and Released Polyacrylamide in Polymer Flooding. *J Beijing Univ Chem Technol* **34** (4): 2007–2414.

Zhang, J. 1995. *The EOR Technology*. Beijing: Petroleum Industry Publishing Company of China.